



Published in final edited form as:

J Comp Neurol. 2016 June 15; 524(9): 1957–1975. doi:10.1002/cne.23984.

The somatosensory brainstem, thalamus, and cortex of the California sea lion (*Zalophus californianus*)

Eva K. Sawyer¹, Emily C. Turner², and Jon H. Kaas²

¹Neuroscience Graduate Program, Vanderbilt University, Nashville, TN, 37240, United States of America

²Department of Psychology, Vanderbilt University, Nashville, TN, 37240, United States of America

Abstract

Pinnipeds (sea lions, seals and walruses) are notable for many reasons, including their ape-sized brains, their adaptation to a coastal niche that combines mastery of the sea with strong ties to land, and the remarkable abilities of their trigeminal whisker system. Yet, little is known about the central nervous system of pinnipeds. Here we report on the somatosensory areas of the nervous system of the California sea lion (*Zalophus californianus*). Using stains for Nissl, cytochrome oxidase, and vesicular glutamate transporters, we investigated the primary somatosensory areas in the brainstem, thalamus and cortex in one sea lion pup, and the external anatomy of the brain in a second pup. We find that the sea lion's impressive array of whiskers is matched by a large trigeminal representation in the brainstem with well-defined parcellation that resembles the barrelettes found in rodents, but scaled up in size. The dorsal column nuclei are large and distinct. The ventral posterior nucleus of the thalamus has divisions, with a large area for the presumptive head representation. Primary somatosensory cortex is located in the neocortex just anterior to the main vertical fissure, and precisely locating it as we do here is useful for comparing the highly gyrified pinniped cortex to other carnivores. To our knowledge this work is the first comprehensive report on the central nervous system areas for any sensory system in a pinniped. The results may be useful in both the veterinary setting and for comparative studies related to brain evolution.

Graphical Abstract

Corresponding author: Eva.k.sawyer@vanderbilt.edu, phone: (917) 535 3700, address: Eva Sawyer, Department of Psychology, Vanderbilt University, PMB 407817, 2301 Vanderbilt Place, Nashville, TN 37240-7817.

Conflict of interest statement: The authors declare no conflicts of interest.

Role of authors: All authors had full access to all the data in the study and take responsibility for the integrity of the data and the accuracy of the data analysis. Study concept and design: EKS. Acquisition of data: EKS and ECT. Analysis and interpretation of data: EKS. Drafting of the manuscript: EKS. Critical revision of the manuscript for important intellectual content: ECT and JHK. Obtained funding: EKS and JHK.



Keywords

sensory system; touch; pinniped; barrelettes; AB_887876; AB_2187552; AB_2313581; AB_2313606

Introduction

California sea lions (*Zalophus californianus*) are members of the order Carnivora, but despite their close phylogenetic relationship to bears, weasels, dogs, and cats, their lifestyle is drastically different (Agnarsson et al., 2010; Song et al., 2012). As members of the otariid (eared seal) clade within pinnipeds, they are semi-aquatic animals that are voracious predators in the water, but are obligately tied to land for parturition and weaning their young (Peterson, 1967). From the wild shorelines of the Pacific to zoos and aquariums worldwide, California sea lions are charismatic animals that are appreciated by humans for their unique behavioral repertoire and extremes of mammalian adaptations.

California sea lions' bodies are built to function both on land and in water, presenting unusual constraints on their musculoskeletal system, sensory systems, and other major organ systems. Independently from the primate lineage they have evolved a brain similar in mass to chimpanzees' (Berta and Sumich, 1999; Herndon et al., 1999; Bininda-Emonds, 2000). They are readily trainable, remarkably agile in water, and are both vocal and social animals (Peterson, 1967; Robards, 1979; Friedman and Leftwich, 2014). As is true for other pinnipeds, sea lions have substantial mystacial vibrissae that are part of a sophisticated touch system we are only beginning to fully appreciate (Dehnhardt, 2008). In the wild, sea lions appear to use their whiskers in social settings by bringing their whiskers in contact with the snout of conspecifics, as if in greeting (Peterson, 1967). It is thought they may also use their whiskers to detect water disturbances caused by potential prey items (Dehnhardt et al., 1998). Sea lion diets show that they are capable of locating fish and squid during dives that

average about 80 m in depth, but these dives can be extend much deeper (274 m) (Fiscus and Baines, 1966; Feldkamp et al., 1989).

In experimental settings, California sea lions are able to use their whiskers to follow the hydrodynamic trail made by a remote controlled submarine creating a wake which mimics that of a fish. California sea lions can still complete this task while blindfolded but not when their vibrissae are blocked by a muzzle (Glaser et al., 2011). California sea lions can also use their whiskers to differentiate the size and shape of objects upon direct contact (Dehnhardt, 1994), and they can manipulate their whiskers to complete complicated sensorimotor tasks (Milne and Grant, 2014).

Despite our knowledge of pinniped behavior and our anthropomorphic interest in the evolution of large brains, little is known about the brains of sea lions. What is known includes a recent report on 1.5 T magnetic resonance imaging of a live California sea lion (Montie et al., 2009) and a body of research on the effect of the toxin domoic acid on the central nervous system of California sea lions, a significant health threat to marine mammals that can mimic symptoms of temporal lobe epilepsy and cause deficits in spatial memory (Scholin et al., 2000; Goldstein et al., 2008; Montie, 2010; Buckmaster et al., 2014; Cook et al., 2015). Meanwhile, other basic questions, such as the anatomy and organization of the major primary sensory areas of the brainstem, thalamus and cortex have remained understudied.

One area of particular interest is the somatosensory system of pinnipeds. First, the highly specialized mystacial whiskers of pinnipeds share many superficial features with the well-studied whisker system in rodents. In rats and mice, the whisker follicles are represented by anatomically distinct modules in the brainstem, thalamus and cortex (Woolsey and Van der Loos, 1970; Van der Loos, 1976; Ma, 1991). As a result, this pathway has become an exemplar of somatotopic mapping in the central nervous system (Fox, 2008). These modules are found in the brainstem in the principal sensory nucleus (PrV), the spinal trigeminal subnucleus interpolaris (SpVi) and the spinal trigeminal subnucleus caudalis (SpVc); in the ventral posterior nucleus (VP) of the thalamus; and in primary somatosensory cortex. It is unknown how the whisker representation is organized in the central nervous system of any pinniped, which all have brains considerably larger than any rodent. It is not obvious that the ~2 g brain of an adult rat should contain the same organizational features as the ~375 g brain of an adult sea lion, especially in light of metabolic and geometric constraints that arise with such extreme scaling of the brain.

Beyond the organization of the representation of the vibrissae follicles, the sea lion has webbed forelimbs, a trait that is rare in mammals. From the digits of primates to raccoons, breaks in skin surfaces are often represented by cell-sparse septa in somatosensory areas of the central nervous system (Welker and Johnson, 1965; Rasmusson, 1988; Strata et al., 2003; Qi et al., 2011). The forelimb/flipper of the sea lion is a limb at the opposite extreme; it is behaviorally important in locomotion but externally the digits are barely recognizable. It is unknown how the forelimb is represented in the sea lion nervous system.

To explore these and other unknown architectonic features, we used various histological stains to investigate the anatomy of the trigeminal nerve, somatosensory brainstem, thalamus and cortex in the California sea lion.

Methods

Animals

Images of live animals in figure 1 were taken at the Central Park Zoo (New York City, NY). Tissue samples were collected from two California sea lion (*Zalophus californianus*) pups (both female, age estimated at 10 months) that were stranded on the California coast during the “unusual mortality event” in the spring of 2015 (Healy, 2015). They were transported to The Marine Mammal Center (Sausalito, CA) for care, where staff veterinarians determined that they had poor clinical prognoses and that euthanasia was the appropriate medical treatment. Veterinary staff euthanized the animals with a barbiturate overdose. The small sample size was dictated by the rare and valuable tissue nature of this tissue. Samples were collected by The Marine Mammal Center under a Marine Mammal Protection Act permit from the National Marine Fisheries Service (no: 18786).

Tissue preservation

The bodies of two sea lion pups were given to after the veterinary staff had declared the animals dead. The bodies were immediately decapitated and flexible rubber tubes were inserted into both carotid arteries and held in place with an adjustable plastic band. The head was then perfused through the carotid arteries via a gravity perfusion with four liters of 0.01 M phosphate buffered saline (PBS), followed by four liters of 4 % paraformaldehyde (PFA) in phosphate buffer (pH 7.5) for a total time of 20 minutes. For both animals no more than 15 minutes passed between the declaration and the beginning of the perfusion. After perfusion, the brain was removed and cranial nerves were sampled bilaterally and stored in 10% formaldehyde. The brains were post-fixed in 4% PFA for 36 hours. One brain was then blocked into 6 pieces; the brainstem, the cerebellum, and the left and right anterior and posterior cortex. Brain tissue blocks were then placed into 30% sucrose (in PB) for at least 3 days for cryo-protection before sectioning. The other brain was kept whole for examination of the external anatomy.

Tissue processing

Segments of cranial nerve V were cut close to the brainstem and post-fixed in 2.5% glutaraldehyde solution in PBS for at least 48 hours. They were then transferred to osmium tetroxide, dehydrated in a graded ethanol series, placed into propylene oxide, and embedded in resin. They were then cut at 1 μ m, mounted onto a glass slide and stained with 1% toluidine blue.

Both sides of each animal’s head were photographed so that the whisker patterns could be compared. From one animal, a section of skin was removed from the whisker pad area. This section was stored in 10% formaldehyde, embedded in paraffin, cut at 5 μ m and then stained for hematoxylin and eosin.

After cryo-protection, the brainstem and the right anterior cortex were cut in coronal sections, while the left anterior cortex was cut in the horizontal plane. The blocks of brain tissue were sectioned at 50 μm using a freezing sliding microtome. The sections were divided into eight series and some series were stained for cytochrome oxidase (CO) (Wong-Riley, 1979), Nissl substance with thionin or vesicular glutamate transporter 1 or 2 protein (VGLUT1, VGLUT2). Nissl preparations were used to identify cell bodies, while the CO preparations revealed areas of elevated metabolic activity. Vesicular glutamate transporters are found in the synaptic vesicles in the terminals of glutamatergic neurons, and thus stains for these proteins label areas of dense terminations of excitatory, glutamatergic axons. Immunohistochemical methods have been previously described elsewhere (Balaram et al., 2013). Stained sections were mounted onto glass slides and coverslipped.

Antibody characterization

Please see table 1 for a list of antibodies used. Rabbit anti-VGLUT1 from Synaptic Systems (Goettingen, Germany) is generated against Strep-Tag® fusion protein of rat VGLUT1 (amino acids 456–560). Preabsorption with the immunogen resulted in negative immunolabeling (Zhou et al., 2007). No staining was observed in VGLUT1 $-/-$ mice (Wojcik et al., 2004). This antibody has been used to label vesicular glutamate transporter 1 in rodents (Dondzillo et al., 2010) and primates (Balaram et al., 2013).

Mouse anti-VGLUT2 from Millipore (USA) is generated against a recombinant rat protein. In Western blots of primate cortex the antibody recognizes a 56-kDa band, which is the known molecular weight of VGLUT2 (Baldwin et al., 2013). This antibody has been used to label vesicular glutamate transporter 2 in rodents (Dondzillo et al., 2010), shrews (Balaram et al., 2013), and primates (Balaram et al., 2013).

In rodents and primates VGLUT1 and VGLUT2 have characteristic expression patterns. Some of these patterns include VGLUT2 being strongly expressed in layer IV of primary sensory areas in mice (Liguz-Leczna and Skangiel-Kramska, 2007), primates (Balaram et al., 2013), and ferrets (Nahmani and Erisir, 2005), whereas VGLUT1 is strongly expressed throughout the neocortex in layers I–III (mice: (Kaneko and Fujiyama, 2002), primates: (Balaram et al., 2013)). In mice the thalamus has a nearly uniform distribution of VGLUT1, but much more discrete distributions of VGLUT2 (Kaneko and Fujiyama, 2002). In addition, in mice immunoreactivity for VGLUT2 is limited to the granular cell layer of the hippocampus, whereas immunoreactivity for VGLUT1 is more distributed throughout the hippocampal layers. The immunostaining we saw for our VGLUT1 and VGLUT2 antibodies in the sea lion tissue matched these previously reported distribution patterns.

Stains for VGLUT1 have also been used to reveal barrelette patterns in the brainstem of mice and other animals (rodents: (Kaneko et al., 2002; Sakurai et al., 2013), primates: (Sawyer et al., 2015)). Stains for VGLUT2 have been used to reveal anatomical patterns in the thalamus of mice and other animals (rodents: (Louderback et al., 2006; Graziano et al., 2008), primates: (Qi et al., 2011; Sawyer et al., 2015)).

Image acquisition and analysis

High-resolution images of the processed tissue were obtained using a SCN400 Slide Scanner (Leica, Germany) or Imager M2 microscope with a mounted AxioCam Mrc (Zeiss, Germany). The images were imported into Adobe Photoshop (Adobe Systems, CA, USA), where they were manipulated only for brightness and contrast.

For the trigeminal nerve counts, 60x images of entire semi-thin sections were imported into Adobe Illustrator (Adobe Systems, CA, USA). We counted every nerve present at two levels of the nerve. A marker was placed on every myelinated fiber. An image of just the markers was imported into ImageJ (Schneider et al., 2012), and counted using the “analyze particles” function. Every nerve in a single section was counted for both the left and right trigeminal nerves. The diameters of a random sample of 1096 nerve fibers were measured to reveal the distribution of the sizes. For the cortical reconstruction, sections stained for CO, VGLUT2 and Nissl were examined. Primary somatosensory cortex was identified as a region with a well-developed layer 4 defined by small cells in Nissl stained sections, and a darkly stained band in the location of layer 4 in CO and VGLUT2 preparations. Sections stained for CO were scanned and the images were imported into Adobe Illustrator. Every 400 μm a cortical section was traced and the regions with a dark CO band were marked. The traces were aligned and major sulci identified. The boundaries of the presumptive somatosensory cortex were identified and the area was plotted on a drawing from a photograph of the juvenile California sea lion brain.

Anatomical designations

Anatomical designations for nuclei and sulci were made with reference to earlier reports in sea lions (Murie, 1874; Montie et al., 2009), their fellow otariid fur seals (Fish, 1898; Ladygina et al., 1985), more distantly related phocid seals (Turner and Miller, 1880; Rioch, 1937), as well as reports on the brains of other carnivores (polar bear [*Urus maritimus*]: (Kappers et al., 1936), raccoon [*Procyon lotor*] (Welker and Seidenstein, 1959; Rasmusson, 1982), dog [*Canis familiaris*] (Singer, 1962), cat [*Felis domesticus*] (Snider and Niemer, 1961)).

Results

Peripheral nervous system

External anatomy of the sea lion—Some of the features of the sea lion body form that are relevant to the organization of their somatosensory representation in the central nervous system are displayed in figure 1. Sea lions have sleek, cylindrically-shaped bodies with a long flexible neck and webbed limbs (fig. 1a, d, e, f). Their forelimbs are broad and powerful (fig. 1a, d, f). The digits are almost completely webbed, and there are no visible nails. The hindlimbs are short compared to its body and can be rotated forward during terrestrial locomotion or can trail behind the body during swimming (fig. 1a, e). The digits of the hindlimb are webbed but the distal tips are separate, and the middle three digits of the hindlimb have nails. Between their hindlimbs, they also have a short, stout tail.

Sea lions have an array of facial vibrissae, with hairs that are long, thick, and straight and found on both their mystacial pad and above their eyes (fig. 1a,b and 2a). They can extend their mystacial whiskers forward, as visible in figure 1c, or lay them back flat against their face. In these specimens some whiskers were blunt at the end, suggestive of recent damage to the array. Of the undamaged whiskers, the shortest mystical whiskers were near the nares (0.3 cm) and the longest were at the ventral caudal extent of the whisker pad (11.5 cm). The average whisker length was 3.0 cm (n= 139). The distribution of the vibrissae was identical on both sides of the face in the two specimens examined such that there were two supraorbital whiskers and the mystacial pad was arranged in six rows with a total of 38 vibrissae (fig. 2b). Row A had four vibrissae, row B had six, rows C–D had eight each, and row F had four. Routine hematoxylin and eosin staining of a single whisker follicle revealed blood cells in the cavernous sinus (fig. 2c), which is a distinguishing feature of vibrissa follicles as opposed to the hair follicles for pelage. The staining also revealed where the deep vibrissal nerve penetrates the dermal capsule.

Trigeminal nerve—The trigeminal nerve was noticeably large compared to the other cranial nerves. The presumptive motor root was distinctive as a separate bundle of fibers that ran adjacent to the thick trigeminal sensory root. Two classes of myelinated fibers were present: those with thick myelin sheaths and those with thin sheaths (see examples in figure 2d). The class of fibers with thin sheaths was 2.58 ± 0.64 μm in diameter (n= 452), while the class of fibers with thick sheaths was larger (8.62 ± 2.65 μm in diameter (n= 643)). The diameter of myelinated axons in the sensory root appeared to segregate into a bimodal distribution with a peak for the thickly myelinated axons (fig. 2g bottom) and another for the thinly myelinated axons (fig. 2g top). There were 118,603 ($\pm 1,834$) myelinated fibers in the sensory root and 3,534 ($\pm 1,90$) myelinated fibers in the motor root. In the sensory root there were 57,248 ($\pm 1,197$) thinly myelinated fibers and 61,355 ($\pm 3,031$) thickly myelinated fibers axons. In the motor root there were 626 (± 141) thinly myelinated fibers and 2,909 (± 49) thickly myelinated fibers axons.

Central nervous system

The ascending somatosensory pathway in mammals has relays in the brainstem, thalamus and cortex. A basic schematic of the connections between the areas that will be discussed in this section is shown in figure 3.

Brainstem

Spinal Trigeminal Nucleus and the Principle Sensory Nucleus: In the SpVc, SpVi, and PrV there was distinct parcellation of the tissue (fig. 4a–d, fig. 4 e–h, and fig. 4i–l, respectively). The Nissl preparations (fig. 4a, e, i) revealed clusters of cells, the CO preparations (fig. 4b, f, j) contained marked modules of high metabolic activity, and the VGLUT1 immunohistochemistry (fig. 4c, g, k) revealed dense termination of nerve afferents. These modules were separated by septa with lower cell density which stained sparsely for CO and VGLUT1 protein. The pattern was similar to the distribution of the whiskers across the surface of the face, though in no single tissue section was there a perfect one-to-one correspondence. In the SpVc, the pattern was visible over 4.2 mm on the rostrocaudal axis (from section 49 to 133), and the average cross-sectional area of the

modules was 66,800 ($\pm 28,000$) μm^2 . In the SpVi, the pattern was visible over 5 mm on the same axis (from section 157 to 257), and the average cross-sectional area of the modules was 34,000 ($\pm 16,200$) μm^2 . In the PrV the pattern was visible over 3.8 mm (from section 393 to 469), and the average cross-sectional area of the modules was 28,900 ($\pm 13,700$) μm^2 .

The Dorsal Column Nuclei: The DCN were present in the dorsomedial medulla as a group of cells with large neuronal cell bodies (fig. 5e, f). These nuclei stained darkly for cytochrome oxidase and VGLUT1 protein (fig. 5g–j), and there were many cell-sparse septa in this nuclear group. The DCN were present from the first sections cut at the level of the caudal SpVc and terminated 10.4 mm rostral to that at the level of the caudal SpVi (sections 1 to 209) (fig. 5k). At the posterior extent of the DCN, a cluster of neurons is distinctly dorsal to the rest of the DCN and is located within the gracile fasciculus (fig. 5e, g, i). However, in sections that are more anterior, this cell group becomes continuous with the gracile nucleus (fig. 5f, j, k). It is unclear if this cell group is best interpreted as Bischoff's nucleus or as a mediodorsal extreme of the gracile nucleus. Here we label it as Bischoff's nucleus and indicate it as distinct from the gracile. The boundaries of the cuneate, gracile, and presumptive Bischoff's nucleus are indicated in figure 5. Finally, within the individual nuclei of the DCN, distinct septa are sometimes present.

Thalamus—In the coronal (fig. 6a–d) and horizontal (fig. 6f–l) sections the VP stains darkly for cytochrome oxidase and VGLUT2 protein. In Nissl-stained sections, the neuronal cell bodies in the VP are larger than those in the surrounding tissue. In the coronal sections, the major subdivision between ventroposterior lateral nucleus (VPL), ventroposterior medial nucleus (VPM) and the ventroposterior inferior nucleus (VPI) could be identified, as shown in the dashed lines in figure 6b–d. Figure 6e illustrates the shifting boundaries of the VPM and VPL throughout the rostrocaudal extent of the VP. A large portion of the VP consists of the VPM, the face representation.

In the horizontal sections the VP nucleus also has a parcellated appearance, which is created by the septa that run through the nucleus. These septa are most visible in the sections stained for VGLUT2 protein, where they can be seen as lightly-stained strips bordered by darkly-stained regions (fig. 6i, l). Septa are also present but less obvious in sections stained for CO and Nissl (fig. 6j and k). Some example septa are marked with arrows in figure 6i–k. These septa could mark boundaries separating the representation of major body regions, but no clearly defined anatomically visible somatotopic map was obvious in the coronal or horizontal planes. The VP was rostrocaudally present over 5 mm in the sections cut in the coronal plane (sections 641 to 745), and dorsoventrally over 6.8 mm in the sections cut in the horizontal plane (sections 529 to 665).

Cortex—The external anatomy of one intact juvenile California sea lion brain was examined. The brain was wider in the parietal/occipital regions than in the frontal regions. It was 6.0 cm wide in the anterior portion, 10.1 cm wide at the widest part of the brain near the posterior end, and 10.2 cm long. The weight after perfusion and immersion fixation was 288.4 g.

The sea lion neocortex has many features typical of carnivorans, but it was notable in the large number of sulci and gyri that are absent in terrestrial members. Distinctive sulci bordering the presumptive somatosensory area are marked in the line drawings in figure 7. The location of the sulci on the two hemispheres was not identical though they were roughly similar (fig. 7a and b). The large cerebellum is found under the occipital lobe. The pseudosylvian sulcus and coronal sulcus are oriented nearly vertically (fig. 7). The anterior portion of the suprasylvian sulcus is not well visible from the external surface but is found on the anterior wall of the convolution labeled as the pseudosylvian sulcus.

The cortex was processed for CO, VGLUT2 protein and Nissl. Some regions of cortex had a distinctive dark band in the sections stained for CO and VGLUT2 protein (fig. 8). This densely-stained band corresponds to layer 4 in the adjacent Nissl-stained sections (fig. 8e–g). In these regions, layer 4 was cell dense, layer 5 was cell sparse, and layer 6 was thick and cell dense (fig. 8f). Together, all these features suggest a primary sensory region of cortex, which in this case appears to be (due to its anterior location) somatosensory cortex.

A series of cortical sections were examined in order to reconstruct the location of the primary somatosensory cortex (S1). The lateral edges of cortical sections 225 to section 681 (spanning 2.23 cm on the rostrocaudal axis) had regions containing the layer 4 band-like features of primary sensory cortex (fig. 9c). At the anterior extent of S1 this band was present dorsolaterally, absent in a mid-lateral segment, and then was again present ventrolaterally. These two segments of S1 united near section 553, and the suprasylvian sulcus served as a ventral boundary. In the horizontal sections, S1 was visible from section 89 to section 805 (spanning 3.58 cm on the dorsoventral axis) (fig. 9d). Most dorsally, S1 was present just anterior to the coronal sulcus. By section 193, S1 extends from the coronal sulcus to the suprasylvian sulcus (which is found within the pseudosylvian fissure), and this pattern is maintained to the ventral extent of the area. The extent of S1 is indicated in figure 9a and b.

Discussion

We present a histological investigation of the primary somatosensory areas in the brainstem, thalamus and cortex of the California sea lion. To our knowledge, this is the first such investigation in any member of the clade Pinnipedia. In light of unusual circumstances affording uncommon access to juvenile sea lions, we were able to preserve the nervous system tissue unusually thoroughly, allowing the histology for markers of metabolism and for specific proteins.

Sea lion whiskers and the trigeminal somatosensory pathway

Our examination of the anatomy of the sea lion whiskers is largely consistent with previous reports (Stephens et al., 1973; Dehnhardt, 1994). Dehnhardt reported that the California sea lions has 38 whiskers in 6 rows, which we also observe, though we find that whiskers are distributed differently within those rows (Dehnhardt, 1994). We found that the 6 rows, from dorsal to ventral, had 4, 6, 8, 8, 8 and 4 whiskers, while Dehnhardt found they had 5, 7, 7, 7, 8 and 4. This could be a real difference in the animals we studied but could also be the result

of the row designation for the short and thin whiskers near the nares, as these are slightly ambiguous.

Our quantification of the myelinated fibers in the trigeminal sensory and motor roots of the sea lion are comparable to a recent study measuring the number of axons in the trigeminal nerve of related Phocid hooded seals (*Cystophora cristata*) and harbor seals (*Phoca vitulina*) (Wohlert et al., 2015). That study reported 166,700 (± 900) myelinated fibers in the sensory root of the trigeminal nerve in the hooded seal and 129,000 ($\pm 3,600$) axons in the same location in the harbor seal. The motor roots for the hooded and harbor seals had 7,600 ($\pm 2,200$) and 7,800 ($\pm 1,100$), respectively. Those estimates for the seal are similar in magnitude to the direct counts of the myelinated fibers in the trigeminal nerve of the California sea lion completed in this study (sensory root = 118,602 (± 1834), motor root = 3534 (± 190)). The larger number of fibers in the trigeminal sensory root of the seals may reflect more refined sensory abilities of the whiskers of seals than of sea lions (ex. (Dehnhardt et al., 2001; Glaser et al., 2011; Murphy, 2013)). However, other factors, such as the size of the animal and the innervation of the rest of the head, are also expected to contribute to those estimates. For example, the number of myelinated fibers in the trigeminal sensory root of a human, which lack a specialized mystacial whisker system, has been estimated at 170,000, with 7,700 axons in the motor root (Pennisi et al., 1991), numbers that are comparable with axons counts reported for pinnipeds. In the future, it may be interesting to investigate the special properties of trigeminal somatosensation in pinnipeds by counting the number of fibers in the maxillary branches of the trigeminal nerve, as this would be a more direct measurement of the innervation of the mystacial vibrissae than counts of the entire trigeminal nerve.

Though not directly comparable in methodology, other researchers have estimated the number of myelinated fibers innervating the whisker pads of other pinnipeds. Based on counting the fibers innervating selected vibrissae and multiplying that by the number of vibrissae the animal has, a single mystacial pad of ringed seals and northern elephant seals are both estimated to have about 160,000 myelinated fibers (Hyvarinen et al., 2009; McGovern et al., 2015), and bearded seals nearly 321,000 (Marshall et al., 2006).

Whiskers have a special place in neuroanatomy, as their representations in the central nervous system provide some of the most stunning examples of somatotopic maps. The best examples come from rodents, where the punctate distributions of vibrissal follicles on the face are replicated in a one-to-one manner in cellular columns in the brainstem, thalamus and cortex. These modules have been termed “barrelettes,” “barreloids,” and “barrels,” respectively (Woolsey and Van der Loos, 1970; Van der Loos, 1976; Belford and Killackey, 1979; Ma, 1991). Here we found a similar pattern of modules in the trigeminal somatosensory nuclei of the brainstem. In the SpVi we found modules that were organized in 6 rows, similar to the 6 rows of whiskers on the sea lion mystacial pad. However, a 6-row organization was less clear in the PrV and SpVc, and in no area did we find 38 modules in the same section. Given the limitations of the material available, this is not surprising. With more samples at the optimal stage of the animal’s development and with tissue sectioned in optimal angles/orientations, it is likely that some sections of the PrV and the SpVi would clearly show 6 rows with a total of 38 modules.

More generally, another remarkable feature of the sea lion brain is its absolute size. The brainstem is interesting in that, though large, the general architecture is still well recognizable compared to smaller mammalian model organisms, such as rats (figure 10). To illustrate these gross similarities, figure 10 shows a comparison between the brainstem of a California sea lion and that of an adult rat. While bigger brainstems are expected in larger animals, larger modules representing the whiskers are not a foregone conclusion. A larger brain must overcome the challenge of needing progressively thicker and longer connections to link areas that are farther apart (Striedter, 2005), and this wiring challenge continues with increasing brain size. One way to solve the problem is to add more, small, functional regions, a solution seen in the cortex of primates (Kaas, 2000). It has been suggested that some cortical modules (e.g., barrels in primary somatosensory cortex, blobs in primary visual cortex, entorhinal clusters, and modules in the dolphin insular cortex) all have a similar cross-sectional area despite the range of overall brain sizes these in which these modules are found (Manger et al., 1998). However, the barrelette-like structures in the sea lion SpVc, SpVi and PrV are 11, 6, and 10 times larger in cross-sectional area than those found in a mouse (Ma, 1991). The presence of such large barrelettes in the sea lion brainstem does not fit the pattern suggested for a limit on the size of modules found in the cortex, and may indicate that the brainstem and cortex evolved under different constraints.

Sea lion limbs and the ascending body representation

Brainstem: The dorsal column nuclei are the site of the first central nervous system synapse for primary somatosensory neurons in the dorsal column-medial lemniscal pathway. These nuclei receive somatosensory input from the neck, forelimb, trunk and hindlimbs. From lateral to medial, the dorsal column nuclei are the cuneate, with sensory input from the upper body; the gracile, with sensory input from the trunk and the hindlimb; and the sometimes-present Bischoff's nucleus, with sensory input from the tail.

The body plan of the sea lion is specialized for its semi-aquatic environment in many ways. The forelimbs of the otariids are unique in marine mammals; unlike dolphins, whales, phocid seals and otters, sea lions and fur seals create thrust for swimming by forcefully bringing their forelimbs together in front of their body (Robards, 1979; Friedman and Leftwich, 2014). Sea lions will also use both their forelimbs and hindlimbs for stability and turning (Robards, 1979). Otariid pinnipeds are also distinct from phocid seals in that they retain the ability to use their forelimbs in terrestrial locomotion.

Here, we report a robust DCN with many cell-sparse septa in the cuneate-gracile complex. It is possible these septa represent a feature of the forelimb/flipper anatomy that is not visible from a gross external inspection but would be apparent if the distribution of somatosensory receptors on the flipper were analyzed more closely. We also report a distinct dorsal-medial cell group at the caudal extent of the gracile nucleus that may be an example of Bischoff's nucleus. Bischoff's nucleus is a DCN found in some animals, and is often associated with the representation of the tail (Johnson et al., 1968; Ostapoff and Johnson, 1988; Sarko et al., 2007). However, sea lions have diminutive tails, so it is surprising to find such a distinct cell group. Without experimental evidence we do not know if this cell group in the expected location of Bischoff's nucleus represents the tail or another body part.

Bischoff's nucleus has been found in other mammals that have independently evolved aquatic lifestyles, such as manatees and whales (Wilson, 1933; Sarko et al., 2007). It is possible that the presence of this distinct cell group is related to a characteristic sensation of swimming that all of these animals experience, perhaps sensing water movements at the caudal end of the body. This could be tested by examining the tail and hind flippers to see if a strong sensory role is likely based on their anatomy, which could be done by looking for high innervation density of, or specialized somatosensory receptors on, these surfaces. It is also possible that the nucleus is related to a reduction in hindlimbs that is seen in marine mammals. Sea lions and fur seals have maintained the ability to use their hind limbs to walk on land, but these hind limbs are reduced compared to their more terrestrial relatives. It would be interesting to look for this brainstem nucleus in the phocidae, members of the pinniped clade that have lost the terrestrial function of their hindlimbs, and which have hind limbs that are more fluke-like. If this nucleus is related to a loss of individuality of the hind limbs we might expect this nucleus to be more pronounced in the phocidae than in the sea lion.

Thalamus—The VP is the main somatosensory nucleus in the thalamus. In mammals, the representation of the head area is more medial in the VPM, and the representation of the body is more lateral in the VPL.

The sea lion VP had lightly stained and cell-poor septa separating more densely stained and cell-dense modules (fig. 6d, h, k). Similar septa are apparent in the VP in other mammalian species. In monkeys and prosimian primates there is a distinct septum separating the hand and face representation, another separating the hand and leg representation, and there are even septa that divide the representations of the digits (Le Gros Clark, 1932; Qi et al., 2011; Sawyer et al., 2015). In the sea lion, the coronal sections have septa that likely represent the forelimb/face border. Based on these septa, the presumptive face representation in the thalamus is large. This result is consistent with the behavioral importance of the whiskers (Dehnhardt, 1994; Glaser et al., 2011; Milne and Grant, 2014), the large trigeminal nerve, the size of the trigeminal representation in the brainstem, and previous electrophysiological mapping in pinniped cortex that reported a large face representation (Ladygina et al., 1985).

With further investigation and additional techniques it should be possible to further divide the sea lion VP complex. In other species, a more cell-dense portion of the VP complex, the ventroposterior superior nucleus, receives proprioceptive input (primates: (Kaas et al., 1984), raccoons: (Wiener et al., 1987) cats: (Dykes et al., 1986)). This division is probably present in the superior portion of the VP complex in sea lions as well. In addition, near the medial extent of the oral cavity representation there should be a parvocellular division of the VPM, an area which has been implicated in taste processing in primates (Iyengar et al., 2007). This would be an interesting area for future work as pinnipeds have non-functional copies of taste receptors involved in the perception of umami and sweet flavors (Jiang et al., 2012; Sato and Wolsan, 2012), which might be reflected in the anatomy of this nucleus.

In addition, in many rodents thalamic barreloids represent the vibrissal follicles (Van der Loos, 1976) and similar whisker-related segmentation has been reported in prosimian primates (Sawyer et al., 2015). However, many of these patterns are best visualized in non-

traditional cutting planes that usually require trial-and-error to perfect (Haidarliu and Ahissar, 2001). In the sea lion thalamus, we hypothesize that there are modules that represent the whisker follicles. However, this investigation is limited to histology of the brain of one animal, and the tissue was cut at traditional coronal and horizontal angles. Thus, the lack of clear whisker-related modules is unsurprising, as it is unlikely we cut the tissue in the optimal angle or orientation for visualization of the VP. It is possible that, within the areas of the VPM with a mottled appearance, such modules would be revealed with further investigation in additional specimens.

Sea Lion Cortex—There have been efforts to describe the external anatomy of sea lion brains (Murie, 1874; Montie et al., 2009), but the many sulci in pinnipeds present a challenge when attempting to identify which cortical landmarks are likely to be homologous to those in other carnivores and which are unique to pinnipeds. Previous anatomical reports in sea lions (Murie, 1874; Montie et al., 2009), fur seals (Ladygina et al., 1985), phocid seals (Rioch, 1937), and other carnivorans (bears (Kappers et al., 1936), raccoons (Welker and Seidenstein, 1959; Rasmusson, 1982), dogs (Singer, 1962), cats (Snider and Niemer, 1961)) were used as references, but in some cases the labeling schemes were in conflict. For example, the location of the ansate sulcus in the otariids (eared seals) is either a branch off the anterior end of the lateral sulcus that does not make contact with the suprasylvian (Ladygina et al. 1986), a short connection between the medial suprasylvian sulcus and the lateral sulcus (Fish, 1898) or it is not labeled (Murie, 1874). Similarly, the coronal sulcus is either a long vertically oriented sulcus that is continuous with the suprasylvian sulcus (Fish, 1898; Ladygina et al., 1985), a diagonally oriented short sulcus that does not come into contact with other sulci (Rioch, 1937), or is not labeled (Murie, 1874). Given these and other conflicts, the labeling of the major sulci was undertaken with caution and limited to those near the presumptive somatosensory cortex.

The sulci patterns for the sea lion and closely related carnivorans are shown in figure 11. The location of S1 is also shown in cats, dogs and raccoons (Bromiley et al., 1956; Welker and Seidenstein, 1959; Dykes et al., 1980; Rasmusson, 1982; Felleman et al., 1983). The species most closely related to pinnipeds for which there is electrophysiological mapping of the somatosensory cortex are the raccoon and domestic dog. In raccoons and dogs, S1 extends between the ansate sulcus dorsally, the coronal sulcus rostrally and the suprasylvian sulcus caudally (Bromiley et al., 1956). In the external examination of the sea lion cortex, S1 appears to extend more caudally compared to other carnivores, stretching all the way to the pseudosylvian sulcus. However, in sections we found that the suprasylvian sulcus is hidden along the rostral bank of the pseudosylvian fissure, and that S1 terminates in that rostral bank. In cats, S1 is more restricted and does not extend to the suprasylvian sulcus. Our finding that S1 in sea lions is roughly bordered by the same sulci as in other carnivoran species lends support to the sulci naming scheme offered here.

Electrophysiological mapping in any pinniped is rare. The most relevant to this study is a multi-unit mapping experiment in a somatosensory area in fur seals (Ladygina et al., 1985). They reported an area that contained an inverted representation of the body so that the tail was represented dorsal and just anterior to the coronal sulcus, the tip of the face was represented just anterior to the pseudosylvian sulcus and the rest of the body was

represented in a somatotopic layout in between. Within this map, the mystacial vibrissae had a large representation that was located just anterior to the pseudosylvian sulcus. This placement is roughly consistent with another investigation in the harbor seal which used surface electrodes to locate a region of cortex that was responsive to taps on the upper lip or mystacial pad (Alderson et al., 1960). Given the phylogenetic distance between sea lions, fur seals, and harbor seals, both of these studies are remarkably consistent with the results reported here. The biggest difference is that Ladygina and colleagues continued to report somatosensory responses to a point slightly more anterior to the coronal sulcus than we have labeled as a primary somatosensory area (Ladygina et al., 1985). This could be the result of using stimuli that would activate proprioceptive afferents, as they are represented in dysgranular area 3a, which is just anterior to S1 in cats (Dykes et al., 1980).

Conclusions

To our knowledge this work represents the most comprehensive examination of the central nervous system representation of a sensory system in any pinniped to date, a group of mammals with unique sensory specializations and large brains. We described the somatosensory regions in the brainstem, thalamus, and cortex. The trigeminal somatosensory system is interesting in a comparative sense to the well-studied rodent trigeminal system, and particularly fascinating in pinnipeds for the remarkable hydrodynamic trail following abilities it facilitates. We show that the face region has a large and distinct representation in the brainstem and thalamus. Our well-defined S1 region in the sea lion helps clarify sulcal homologies between the gyrified brains of pinnipeds and terrestrial carnivores. Here we show that despite the great phenotypic differences between mice and California sea lions, many fundamental aspects of central nervous system organization are shared.

Acknowledgments

Funding: NIH grant NS084706 to EKS and NIH grant NS016446 to JHK

This work could not have taken place without the assistance of the research staff and veterinarians at The Marine Mammal Center and we thank them for their assistance and flexibility. The EM samples were prepared in part through the use of the Vanderbilt University Medical Center Cell Imaging Shared Resource. In addition, the histology of the whisker follicle was prepared by Vanderbilt University Medical Center's Translational Pathology Shared Resource, and some images were visualized using the Digital Histology Shared Resource. We thank Lauren Trice for her significant and dedicated assistance with the histology for this large brain. We thank Duncan Leitch and Nina Patzke for their intellectual contributions and technical assistance. This work was funded by NIH grant NS016446 to JHK and NIH grant NS084706 to EKS, and a dissertation enhancement grant from the Vanderbilt University Graduate School to EKS.

Literature Cited

- Agnarsson I, Kuntner M, May-Collado LJ. Dogs, cats, and kin: a molecular species-level phylogeny of Carnivora. *Molecular phylogenetics and evolution*. 2010; 54(3):726–745. [PubMed: 19900567]
- Alderson AM, Diamantopoulos E, Downman CB. Auditory cortex of the seal (*Phoca vitulina*). *Journal of anatomy*. 1960; 94:506–511. [PubMed: 13682212]
- Balaran P, Hackett TA, Kaas JH. Differential expression of vesicular glutamate transporters 1 and 2 may identify distinct modes of glutamatergic transmission in the macaque visual system. *Journal of chemical neuroanatomy*. 2013; 50–51:21–38. [PubMed: 19594444]

- Baldwin MK, Balam P, Kaas JH. Projections of the superior colliculus to the pulvinar in prosimian galagos (*Otolemur garnettii*) and VGLUT2 staining of the visual pulvinar. *The Journal of comparative neurology*. 2013; 521(7):1664–1682. [PubMed: 23124867]
- Belford GR, Killackey HP. The development of vibrissae representation in subcortical trigeminal centers of the neonatal rat. *The Journal of comparative neurology*. 1979; 188(1):63–74. [PubMed: 500854]
- Berta, A.; Sumich, JL. *Marine mammals : evolutionary biology*. San Diego: Academic Press; 1999. Integumentary and sensory systems; p. xiiip. 494
- Bininda-Emonds ORP. Pinniped brain sizes. *Marine Mammal Science*. 2000; 16(2):469–481.
- Bromiley RB, Pinto Hamuy T, Woolsey CN. Somatic afferent areas I and II of dog's cerebral cortex. *Journal of neurophysiology*. 1956; 19(6):485–499. [PubMed: 13377199]
- Buckmaster PS, Wen X, Toyoda I, Gulland FM, Van Bonn W. Hippocampal neuropathology of domoic acid-induced epilepsy in California sea lions (*Zalophus californianus*). *The Journal of comparative neurology*. 2014; 522(7):1691–1706. [PubMed: 24638960]
- Cook PF, Reichmuth C, Rouse AA, Libby LA, Dennison SE, Carmichael OT, Kruse-Elliott KT, Bloom J, Singh B, Fravel VA, Barbosa L, Stuppino JJ, Van Bonn WG, Gulland FM, Ranganath C. Algal toxin impairs sea lion memory and hippocampal connectivity, with implications for strandings. *Science*. 2015; 350(6267):1545–1547. [PubMed: 26668068]
- Dehnhardt G. Tactile size discrimination by a California sea lion (*Zalophus californianus*) using its mystacial vibrissae. *Journal of comparative physiology A, Sensory, neural, and behavioral physiology*. 1994; 175(6):791–800.
- Dehnhardt G, Mauck B, Bleckmann H. Seal whiskers detect water movements. *Nature*. 1998; 394(6690):235–236.
- Dehnhardt G, Mauck B, Hanke W, Bleckmann H. Hydrodynamic trail-following in harbor seals (*Phoca vitulina*). *Science*. 2001; 293(5527):102–104. [PubMed: 11441183]
- Dehnhardt, GMB. *Sensory Evolution on the Threshold: Adaptations in Secondarily Aquatic Vertebrates*. 2008. Mechanoreception in secondarily aquatic vertebrates; p. 295-314.
- Dondzillo A, Satzler K, Horstmann H, Altrock WD, Gundelfinger ED, Kuner T. Targeted three-dimensional immunohistochemistry reveals localization of presynaptic proteins Bassoon and Piccolo in the rat calyx of Held before and after the onset of hearing. *The Journal of comparative neurology*. 2010; 518(7):1008–1029. [PubMed: 20127803]
- Dykes RW, Herron P, Lin CS. Ventroposterior thalamic regions projecting to cytoarchitectonic areas 3a and 3b in the cat. *Journal of neurophysiology*. 1986; 56(6):1521–1541. [PubMed: 3027273]
- Dykes RW, Rasmusson DD, Hoeltzell PB. Organization of primary somatosensory cortex in the cat. *Journal of neurophysiology*. 1980; 43(6):1527–1546. [PubMed: 7411175]
- Feldkamp SD, DeLong RL, Antonelis GA. Diving patterns of California sea lions, *Zalophus californianus*. *Canadian Journal of Zoology*. 1989; 67(4):872–883.
- Felleman DJ, Wall JT, Cusick CG, Kaas JH. The representation of the body surface in S-I of cats. *The Journal of neuroscience : the official journal of the Society for Neuroscience*. 1983; 3(8):1648–1669. [PubMed: 6875661]
- Fiscus CH, Baines GA. Food and Feeding Behavior of Steller and California Sea Lions. *Journal of Mammalogy*. 1966; 47(2):195–200.
- Fish PA. The brain of the fur seal, *Callorhinus ursinus*; with a comparative description of those of *Zalophus californianus*, *Phoca vitulina*, *Ursus americanus* and *Monachus tropicalis*. *Journal of Comparative Neurology*. 1898; 8(1–2):57–91.
- Fox, K. *Barrel Cortex*. New York: Cambridge University Press; 2008.
- Friedman C, Leftwich MC. The kinematics of the California sea lion foreflipper during forward swimming. *Bioinspiration & Biomimetics*. 2014; 9(4):046010. [PubMed: 25378293]
- Glaser N, Wieskotten S, Otter C, Dehnhardt G, Hanke W. Hydrodynamic trail following in a California sea lion (*Zalophus californianus*). *Journal of comparative physiology A, Neuroethology, sensory, neural, and behavioral physiology*. 2011; 197(2):141–151.
- Goldstein T, Mazet JA, Zabka TS, Langlois G, Colegrove KM, Silver M, Bargu S, Van Dolah F, Leighfield T, Conrad PA, Barakos J, Williams DC, Dennison S, Haulena M, Gulland FM. Novel symptomatology and changing epidemiology of domoic acid toxicosis in California sea lions

- (*Zalophus californianus*): an increasing risk to marine mammal health. *Proceedings Biological sciences / The Royal Society*. 2008; 275(1632):267–276. [PubMed: 18006409]
- Graziano A, Liu XB, Murray KD, Jones EG. Vesicular glutamate transporters define two sets of glutamatergic afferents to the somatosensory thalamus and two thalamocortical projections in the mouse. *The Journal of comparative neurology*. 2008; 507(2):1258–1276. [PubMed: 18181146]
- Haidarliu S, Ahissar E. Size gradients of barreloids in the rat thalamus. *The Journal of comparative neurology*. 2001; 429(3):372–387. [PubMed: 11116226]
- Healy, J. *The New York Times*. 2015. Starving Sea Lions Washing Ashore by the Hundreds in California; p. A12
- Herndon JG, Tigges J, Anderson DC, Klumpp SA, McClure HM. Brain weight throughout the life span of the chimpanzee. *The Journal of comparative neurology*. 1999; 409(4):567–572. [PubMed: 10376740]
- Hyvarinen H, Palviainen A, Strandberg U, Holopainen IJ. Aquatic environment and differentiation of vibrissae: comparison of sinus hair systems of ringed seal, otter and pole cat. *Brain, behavior and evolution*. 2009; 74(4):268–279.
- Iyengar S, Qi HX, Jain N, Kaas JH. Cortical and thalamic connections of the representations of the teeth and tongue in somatosensory cortex of new world monkeys. *The Journal of comparative neurology*. 2007; 501(1):95–120. [PubMed: 17206603]
- Jiang P, Josue J, Li X, Glaser D, Li W, Brand JG, Margolskee RF, Reed DR, Beauchamp GK. Major taste loss in carnivorous mammals. *Proceedings of the National Academy of Sciences of the United States of America*. 2012; 109(13):4956–4961. [PubMed: 22411809]
- Johnson JI Jr, Welker WI, Pubols BH Jr. Somatotopic organization of raccoon dorsal column nuclei. *The Journal of comparative neurology*. 1968; 132(1):1–43. [PubMed: 4378068]
- Kaas JH. Why is Brain Size so Important: Design Problems and Solutions as Neocortex Gets Bigger or Smaller. *Brain and Mind*. 2000; 1(1):7–23.
- Kaas JH, Nelson RJ, Sur M, Dykes RW, Merzenich MM. The somatotopic organization of the ventroposterior thalamus of the squirrel monkey, *Saimiri sciureus*. *The Journal of comparative neurology*. 1984; 226(1):111–140. [PubMed: 6736292]
- Kaneko T, Fujiyama F. Complementary distribution of vesicular glutamate transporters in the central nervous system. *Neuroscience research*. 2002; 42(4):243–250. [PubMed: 11985876]
- Kaneko T, Fujiyama F, Hioki H. Immunohistochemical localization of candidates for vesicular glutamate transporters in the rat brain. *The Journal of comparative neurology*. 2002; 444(1):39–62. [PubMed: 11835181]
- Kappers, CUA.; Huber, GC.; Crosby, EC. *The comparative anatomy of the nervous system of vertebrates, including man*. New York: Macmillan; 1936.
- Ladygina TF, Popov VV, Supin AY. Topical organization of somatic projections in the fur seal cerebral cortex. *Neurophysiology*. 1985; 17(3):246–252.
- Le Gros Clark WE. The structure and function of the thalamus. *Brain : a journal of neurology*. 1932; 55(3):406–470.
- Liguz-Leczna M, Skangiel-Kramska J. Vesicular glutamate transporters VGLUT1 and VGLUT2 in the developing mouse barrel cortex. *International journal of developmental neuroscience : the official journal of the International Society for Developmental Neuroscience*. 2007; 25(2):107–114. [PubMed: 17289331]
- Louderback KM, Glass CS, Shamalla-Hannah L, Erickson SL, Land PW. Subbarrel patterns of thalamocortical innervation in rat somatosensory cortical barrels: Organization and postnatal development. *The Journal of comparative neurology*. 2006; 497(1):32–41. [PubMed: 16680781]
- Ma PM. The barrelettes--architectonic vibrissal representations in the brainstem trigeminal complex of the mouse. I. Normal structural organization. *The Journal of comparative neurology*. 1991; 309(2):161–199. [PubMed: 1715890]
- Manger P, Sum M, Szymanski M, Ridgway SH, Krubitzer L. Modular subdivisions of dolphin insular cortex: does evolutionary history repeat itself? *Journal of cognitive neuroscience*. 1998; 10(2):153–166. [PubMed: 9555104]
- Marshall CD, Amin H, Kovacs KM, Lydersen C. Microstructure and innervation of the mystacial vibrissal follicle-sinus complex in bearded seals, *Erignathus barbatus* (Pinnipedia: Phocidae). *The*

anatomical record Part A, Discoveries in molecular, cellular, and evolutionary biology. 2006; 288(1):13–25.

- McGovern KA, Marshall CD, Davis RW. Are vibrissae viable sensory structures for prey capture in northern elephant seals, *Mirounga angustirostris*? *Anatomical record*. 2015; 298(4):750–760.
- Milne AO, Grant RA. Characterisation of whisker control in the California sea lion (*Zalophus californianus*) during a complex, dynamic sensorimotor task. *Journal of comparative physiology A, Neuroethology, sensory, neural, and behavioral physiology*. 2014; 200(10):871–879.
- Montie EW, Pussini N, Schneider GE, Battey TW, Dennison S, Barakos J, Gulland F. Neuroanatomy and volumes of brain structures of a live California sea lion (*Zalophus californianus*) from magnetic resonance images. *Anatomical record*. 2009; 292(10):1523–1547.
- Montie EW, Pussini N, Battey TW, Barakos J, Dennison S, Colegrove K, Gulland F. Magnetic resonance imaging quality and volumes of brain structures from live and postmortem imaging of California sea lions with clinical signs of domoic acid toxicosis. *Diseases of aquatic organisms*. 2010; 91(3):243–256. [PubMed: 21133324]
- Murie J. Researches upon the Anatomy of the Pinnipedia.—Part III. Descriptive Anatomy of the Sea-lion (*Otaria jubata*). *The Transactions of the Zoological Society of London*. 1874; 8(9):501–582.
- Murphy, CT. Structure and Function of Pinniped Vibrissae. 2013.
- Nahmani M, Erisir A. VGLuT2 immunohistochemistry identifies thalamocortical terminals in layer 4 of adult and developing visual cortex. *The Journal of comparative neurology*. 2005; 484(4):458–473. [PubMed: 15770654]
- Ostapoff EM, Johnson JI. Distribution of cells projecting to thalamus vs. those projecting to cerebellum in subdivisions of the dorsal column nuclei in raccoons. *The Journal of comparative neurology*. 1988; 267(2):211–230. [PubMed: 3343398]
- Pennisi E, Cruccu G, Manfredi M, Palladini G. Histometric study of myelinated fibers in the human trigeminal nerve. *Journal of the neurological sciences*. 1991; 105(1):22–28. [PubMed: 1795166]
- Peterson, RSB.; GA. The natural history and behaviour of the California sea lion. Stillwater, OK, USA: American Society of Mammalogists; 1967.
- Qi HX, Gharbawie OA, Wong P, Kaas JH. Cell-poor septa separate representations of digits in the ventroposterior nucleus of the thalamus in monkeys and prosimian galagos. *The Journal of comparative neurology*. 2011; 519(4):738–758. [PubMed: 21246552]
- Rasmusson DD. Reorganization of raccoon somatosensory cortex following removal of the fifth digit. *The Journal of comparative neurology*. 1982; 205(4):313–326. [PubMed: 7096623]
- Rasmusson DD. Projections of digit afferents to the cuneate nucleus in the raccoon before and after partial deafferentation. *The Journal of comparative neurology*. 1988; 277(4):549–556. [PubMed: 2463292]
- Rioch DM. A physiological and histological study of the frontal cortex of the seal (*Phoca vitulina*). *The Biological Bulletin*. 1937; 73(3):591–602.
- Robards MJ. Somatic neurons in the brainstem and neocortex projecting to the external nucleus of the inferior colliculus: an anatomical study in the opossum. *The Journal of comparative neurology*. 1979; 184(3):547–565. [PubMed: 422756]
- Sakurai K, Akiyama M, Cai B, Scott A, Han BX, Takatoh J, Sigrist M, Arber S, Wang F. The organization of submodality-specific touch afferent inputs in the vibrissa column. *Cell reports*. 2013; 5(1):87–98. [PubMed: 24120861]
- Sarko DK, Johnson JI, Switzer RC 3rd, Welker WI, Reep RL. Somatosensory nuclei of the manatee brainstem and thalamus. *Anatomical record*. 2007; 290(9):1138–1165.
- Sato JJ, Wolsan M. Loss or major reduction of umami taste sensation in pinnipeds. *Naturwissenschaften*. 2012; 99(8):655–659. [PubMed: 22777285]
- Sawyer EK, Liao CC, Qi HX, Balaram P, Matrov D, Kaas JH. Subcortical barrelette-like and barrelloid-like structures in the prosimian galago (*Otolemur garnetti*). *Proceedings of the National Academy of Sciences of the United States of America*. 2015; 112(22):7079–7084. [PubMed: 26038561]
- Schneider CA, Rasband WS, Eliceiri KW. NIH Image to ImageJ: 25 years of image analysis. *Nature methods*. 2012; 9(7):671–675. [PubMed: 22930834]
- Scholin CA, Gulland F, Doucette GJ, Benson S, Busman M, Chavez FP, Cordaro J, DeLong R, De Vogelaere A, Harvey J, Haulena M, Lefebvre K, Lipscomb T, Loscutoff S, Lowenstine LJ, Marin

- R 3rd, Miller PE, McLellan WA, Moeller PD, Powell CL, Rowles T, Silvagni P, Silver M, Spraker T, Trainer V, Van Dolah FM. Mortality of sea lions along the central California coast linked to a toxic diatom bloom. *Nature*. 2000; 403(6765):80–84. [PubMed: 10638756]
- Singer, M. Philadelphia: Saunders. 1962. The brain of the dog in section; p. xvp. x1124 plates
- Snider, RS.; Niemer, WT. A stereotaxic atlas of the cat brain. Chicago: University of Chicago Press; 1961.
- Song S, Liu L, Edwards SV, Wu S. Resolving conflict in eutherian mammal phylogeny using phylogenomics and the multispecies coalescent model. *Proceedings of the National Academy of Sciences of the United States of America*. 2012; 109(37):14942–14947. [PubMed: 22930817]
- Stephens RJ, Beebe IJ, Poulter TC. Innervation of the vibrissae of the California sea lion, *Zalophus californianus*. *The Anatomical record*. 1973; 176(4):421–441. [PubMed: 4723405]
- Strata F, Coq JO, Kaas JH. The chemo- and somatotopic architecture of the Galago cuneate and gracile nuclei. *Neuroscience*. 2003; 116(3):831–850. [PubMed: 12573723]
- Striedter, GF. Principles of brain evolution. Sunderland, Mass: Sinauer Associates; 2005. p. xiip. 436
- Turner, W.; Miller, WCS. Report on the seals collected during the voyage of H. M. S. Challenger in the years 1873–76. Edinburgh; 1880.
- Van der Loos H. Barreloids in mouse somatosensory thalamus. *Neuroscience letters*. 1976; 2(1):1–6. [PubMed: 19604804]
- Welker WI, Johnson JI. Correlation between Nuclear Morphology and Somatotopic Organization in Ventro-Basal Complex of the Raccoon's Thalamus. *Journal of anatomy*. 1965; 99:761–790. [PubMed: 5325779]
- Welker WI, Seidenstein S. Somatic sensory representation in the cerebral cortex of the racoon (*Procyon lotor*). *The Journal of comparative neurology*. 1959; 111:469–501. [PubMed: 13843838]
- Wiener SI, Johnson JI, Ostapoff EM. Organization of postcranial kinesthetic projections to the ventrobasal thalamus in raccoons. *The Journal of comparative neurology*. 1987; 258(4):496–508. [PubMed: 3108336]
- Wilson RB. The anatomy of the brain of the whale (*Balaenoptera sulfurea*). *The Journal of comparative neurology*. 1933; 58(2):419–480.
- Wohlert D, Kroger J, Witt M, Schmitt O, Wree A, Czech-Damal N, Siebert U, Folkow L, Hanke FD. A Comparative Morphometric Analysis of Three Cranial Nerves in Two Phocids: The Hooded Seal (*Cystophora Cristata*) and the Harbor Seal (*Phoca Vitulina*). *Anatomical record*. 2015
- Wojcik SM, Rhee JS, Herzog E, Sigler A, Jahn R, Takamori S, Brose N, Rosenmund C. An essential role for vesicular glutamate transporter 1 (VGLUT1) in postnatal development and control of quantal size. *Proceedings of the National Academy of Sciences of the United States of America*. 2004; 101(18):7158–7163. [PubMed: 15103023]
- Wong-Riley M. Changes in the visual system of monocularly sutured or enucleated cats demonstrable with cytochrome oxidase histochemistry. *Brain research*. 1979; 171(1):11–28. [PubMed: 223730]
- Woolsey TA, Van der Loos H. The structural organization of layer IV in the somatosensory region (SI) of mouse cerebral cortex. The description of a cortical field composed of discrete cytoarchitectonic units. *Brain research*. 1970; 17(2):205–242. [PubMed: 4904874]
- Zhou J, Nannapaneni N, Shore S. Vesicular glutamate transporters 1 and 2 are differentially associated with auditory nerve and spinal trigeminal inputs to the cochlear nucleus. *The Journal of comparative neurology*. 2007; 500(4):777–787. [PubMed: 17154258]



Figure 1.

The California sea lion. **(A)** An adult female rests on a rock, displaying the full body of a sea lion. **(B)** The whisker pad on a sea lion. **(C)** Two sea lions move their whiskers towards the other in greeting. **(D)** The long forelimbs of the sea lion is nearly completely webbed. The forelimbs are used for propulsion when swimming. **(E)** The hind limb and tail of the sea lion. The hindlimb is webbed but has 5 distinct digits at the distal end of the limb. Hindlimbs are used during swimming for directional corrections, and can be rotated forward for walking or sitting when on land. **(F)** A sea lion displaying its long flexible neck.

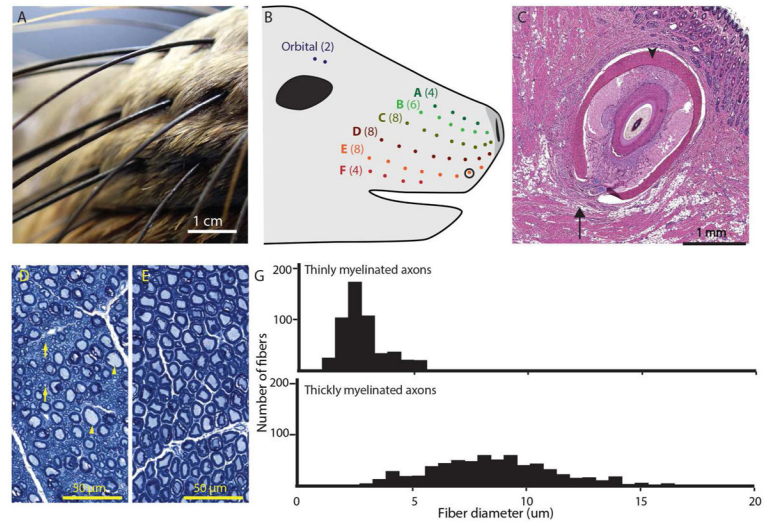


Figure 2.

The peripheral trigeminal somatosensory system of the California sea lion. **(A)** A photo of the mystacial vibrissae. **(B)** A diagram of the location of the vibrissae on the head of the sea lion. **(C)** A longitudinal section of the whisker follicle circled in B that has been stained for hematoxylin and eosin. The arrow points to the deep vibrissal nerve that innervated the base of the follicle. The arrowhead indicates the location of blood cells in the cavernous sinus, a feature of whisker follicles. **(D)** A photomicrograph of the sensory root of the trigeminal nerve stained with toluidine blue. Arrowheads point to examples of large fibers, and arrows point to examples of small fibers. **(E)** A photomicrograph of the motor root of the trigeminal nerve stained with toluidine blue. **(F)** Histograms of the bimodal distribution of axon diameters in the sensory root of the trigeminal nerve of thinly myelinated (top) and thickly myelinated (bottom) fibers.

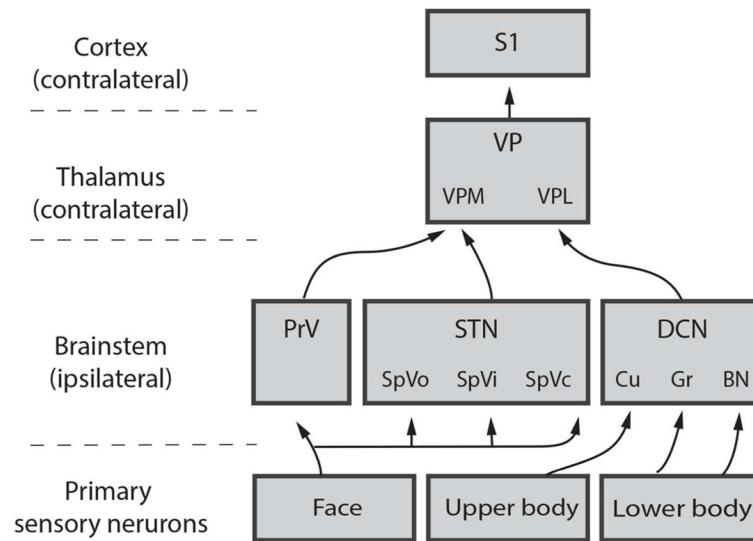


Figure 3.

A basic schematic of the lemniscal somatosensory pathway. Abbreviations: BN= Bischoff's nucleus, Cu= cuneate, DCN= dorsal column nucleus, Gr= gracile nucleus, PrV= principal sensory nucleus, S1= primary somatosensory nucleus; STN= spinal trigeminal nucleus, SpVc= spinal trigeminal subnucleus caudalis, SpVi= spinal trigeminal subnucleus interpolaris, SpVo= spinal trigeminal subnucleus oralis, VP= ventroposterior nucleus, VPL= ventroposterior lateral subnucleus, VPM= ventroposterior medial subnucleus.

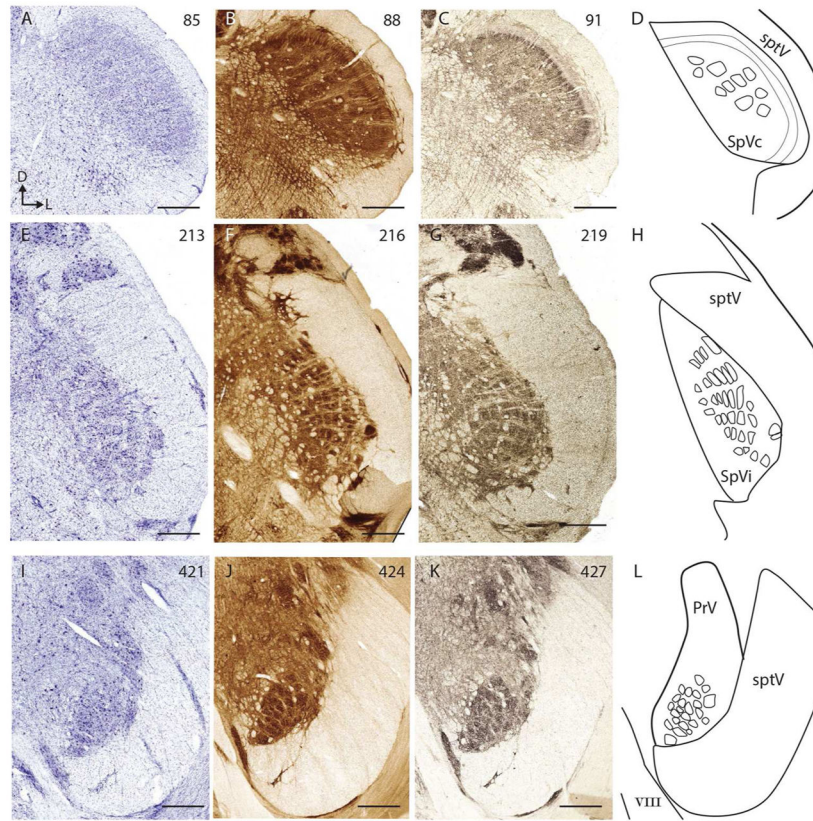


Figure 4. The trigeminal brainstem of the California sea lion. **(A)**, **(B)** and **(C)**: Photomicrographs of sections of the spinal trigeminal subnucleus caudalis stained for Nissl substance, cytochrome oxidase (CO) and vesicular glutamate transporter 1 (VGLUT1), respectively. **(D)** A sketch indicating the location of modules in **B**. **(E)**, **(F)** and **(G)**: Photomicrographs of sections of the spinal trigeminal subnucleus interpolaris, stained as in **A**, **B**, and **C**. **(H)** A sketch indicating the location of modules in **F**. **(I)**, **(J)** and **(K)**: Photomicrographs of sections of the principal sensory nucleus, stained as in **A**, **B**, and **C**. **(L)** A sketch indicating the location of modules in **I**. In all parts of the figure the number of the section is indicated in the upper right and dorsal is up whereas lateral is to the right. Scale bar = 1 mm. All sections are oriented as shown in **A**. Abbreviations: VIII= 8TH cranial nerve, D= dorsal, L= lateral, PrV= principal sensory nucleus, SpVc= spinal trigeminal subnucleus caudalis, SpVi= spinal trigeminal subnucleus interpolaris, SpVt= spinal trigeminal tract.

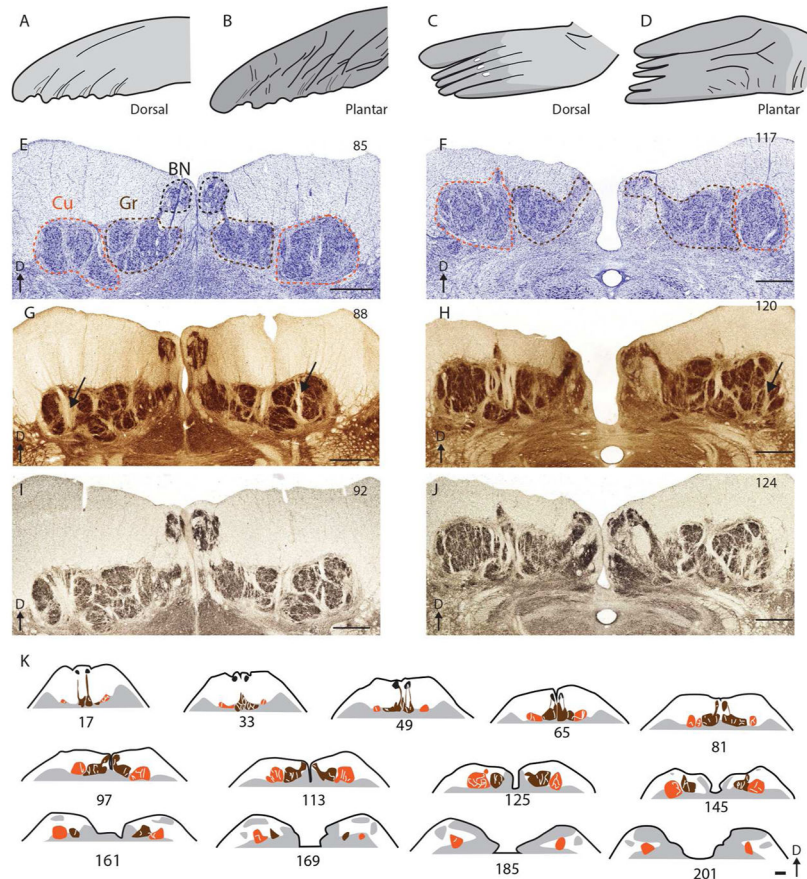


Figure 5.

The dorsal column nuclei (DCN) of the California sea lion. (A) and (B): Sketch of the forelimb of a sea lion. (C) and (D): Sketch of the hindlimb of a sea lion. (E) and (F): Photomicrographs of the DCN stained for Nissl substance. The number of the section is indicated in the upper right. The cuneate, gracile, and Bischoff's nucleus is outlined in dotted lines of orange, brown and black, respectively. (G) and (H): Photomicrographs of the cuneate-gracile complex stained for cytochrome oxidase, labeled as in A and B. (I) and (J): Photomicrographs of the cuneate-gracile complex stained for vesicular glutamate transporter 1, labeled as in A and B (K): Sketches of the cuneate-gracile complex showing the throughout its rostral caudal extent, from section 17 (most caudal) to 201 (most rostral). The cuneate, gracile, and Bischoff's nucleus are colored orange, brown and black, respectively. Scale bar = 1 mm. Abbreviations: BN= Bischoff's nucleus, Cu= cuneate nucleus, D= dorsal, Gr= gracile nucleus.

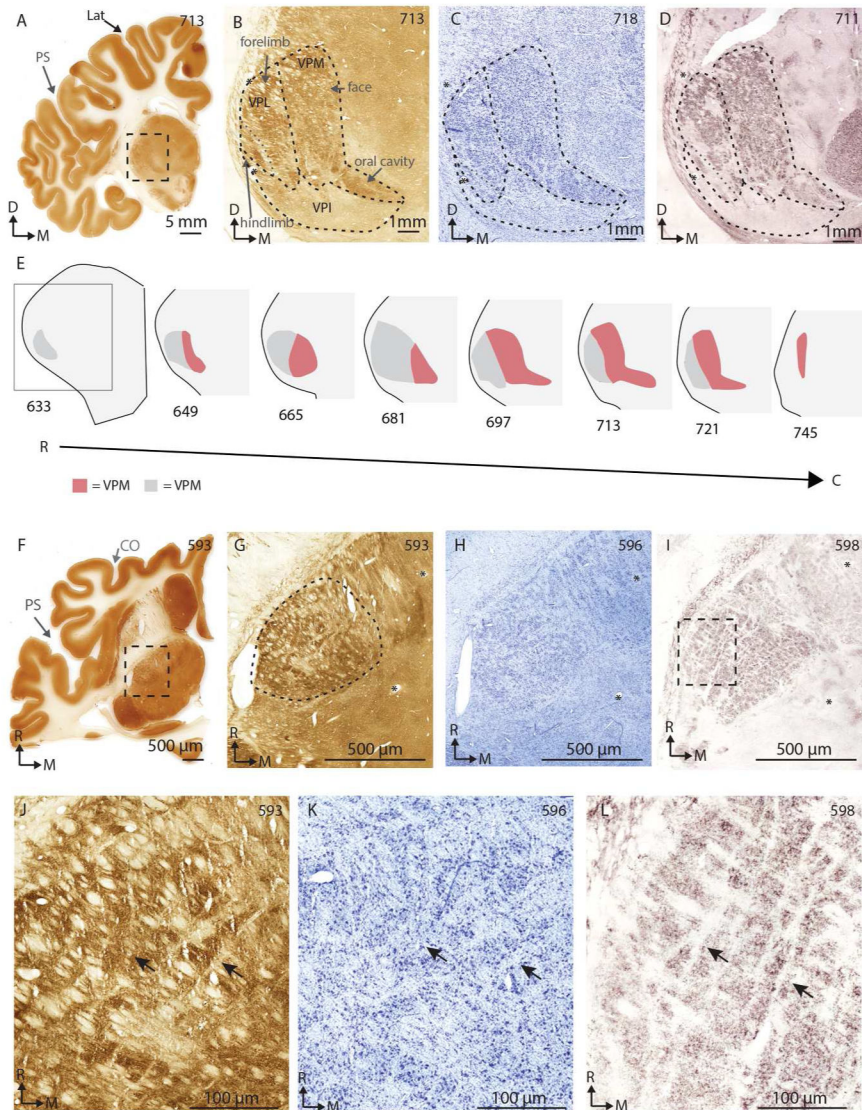


Figure 6.

The somatosensory thalamus of the California sea lion. (A) A photomicrograph of a coronal section of the anterior cortex, stained for cytochrome oxidase. The area outlined by the dashed line is seen in B, C and D. (B), (C) and (D): Photomicrographs of matched sections of the thalamus that have been cut in the coronal plane and stained for cytochrome oxidase, Nissl and vesicular glutamate transporter 2 (VGLUT2), respectively. The areas outlined by the dotted lines are the ventroposterior medial subnucleus (VPM), the ventroposterior lateral subnucleus (VPL) and the ventral posterior inferior nucleus (VPI). Asterisk mark matching blood vessels. (E) Traces of the ventroposterior nucleus in a series of coronal sections, showing the relative contributions of the VPM and VPL across the rostral-caudal axis. The VPM, the area representing the head region, is shaded red while the VPL is shaded in grey. (F) A photomicrograph of a horizontal section of the anterior cortex, stained for cytochrome oxidase. The area outlined by the dashed line is seen in F, G and H. (G), (H) and (I) A photomicrograph of matched sections of the thalamus that have been cut in the horizontal

plane and stained for cytochrome oxidase, Nissl, and VGLUT2. Asterix mark matching blood vessels. The area outlined by the dotted line in F is the VP. The area outlined by the dashed line in I is seen in J, K, and L. (**J**), (**K**) and (**L**), matched images of a central region of the ventroposterior nucleus, as seen in F–H but at a higher magnification. Arrows indicate septa. In all parts of the figure the number of the section is indicated in the upper right. Abbreviations: C= caudal, CO= coronal sulcus, D= dorsal, Lat= lateral sulcus, M= medial, Ps= pseudosylvian sulcus, R= rostral.

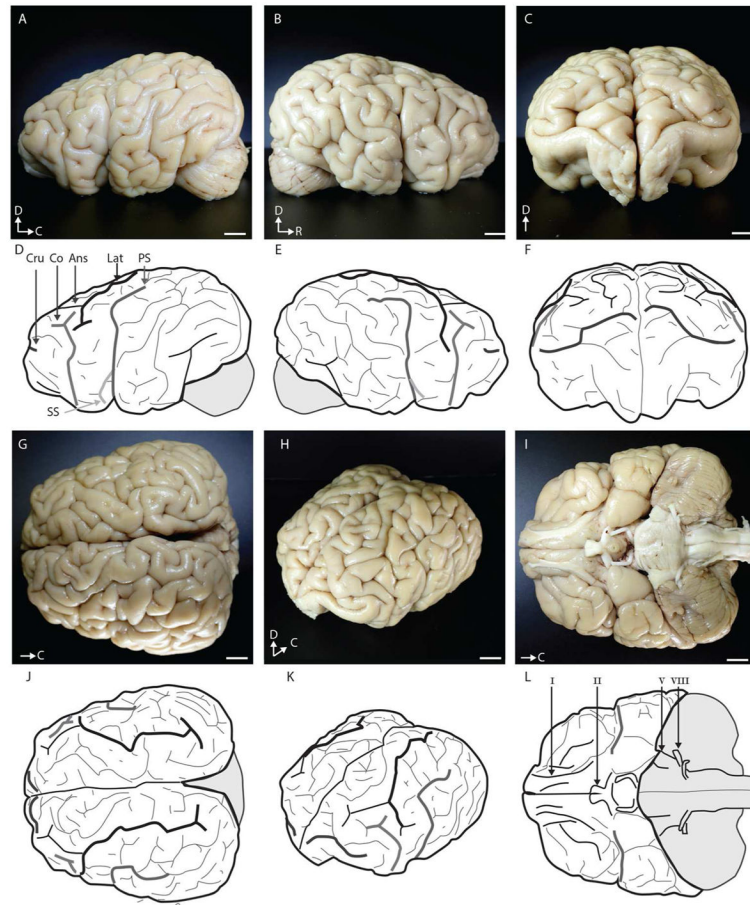


Figure 7.

The external anatomy of the brain of the California sea lion. **(A)**, **(B)** and **(C)**: A left lateral, right lateral, and frontal view, respectively. **(D)**, **(E)**, and **(F)**: A drawing of A, B and C, with 4 major sulci labeled. **(G)**, **(H)** and **(I)**: A dorsal, isometric, and ventral view, respectively. **(J)**, **(K)** and **(L)**: A drawing of G, H and I with the same major sulci highlighted as in D, E and F. In addition, the sensory cranial nerves are labeled in L. Scale bar = 1 cm. Abbreviations: Ans= ansate sulcus C= caudal, Co= coronal sulcus, Cr= cruciate sulcus, D= dorsal, Lat= lateral sulcus, Ps= pseudosylvian sulcus, R= rostral, SS= suprasylvian sulcus.

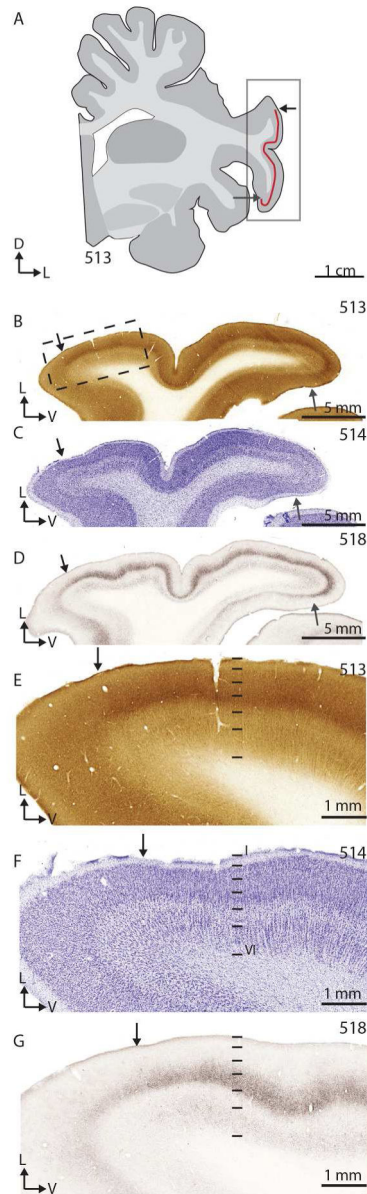


Figure 8.

Example histology on coronal sections of the anterior sea lion cortex. **(A)** A schematic of sections 513–518. The red line is the area where the presumptive primary somatosensory cortex is, as defined in sections stained for cytochrome oxidase (CO), Nissl, and vesicular glutamate transporter 2 protein (VGLUT2). The grey line indicates the area enlarged in B, C, and D. Arrows point to the borders of the histologically defined area. **(B)**: Section 513, stained for cytochrome oxidase, showing a dark brown stripe in layer 4. The dashed line indicates the area enlarged in E, F and G **(C)**: Section 514, stained for Nissl substance, showing a neuron dense layer 4 and 6 and a neuron sparse layer 5. **(D)** Section 518, stained for VGLUT2, showing dense labeling corresponding to layer 4, and more sparse labeling corresponding to layer 6. **(E)**, **(F)** and **(G)** Enlarged sections of B, C, and D. Black

horizontal lines indicate the boundaries of the layers as defined by cytoarchitecture in F.
Abbreviations: D= dorsal, L= lateral, V= ventral.

Author Manuscript

Author Manuscript

Author Manuscript

Author Manuscript

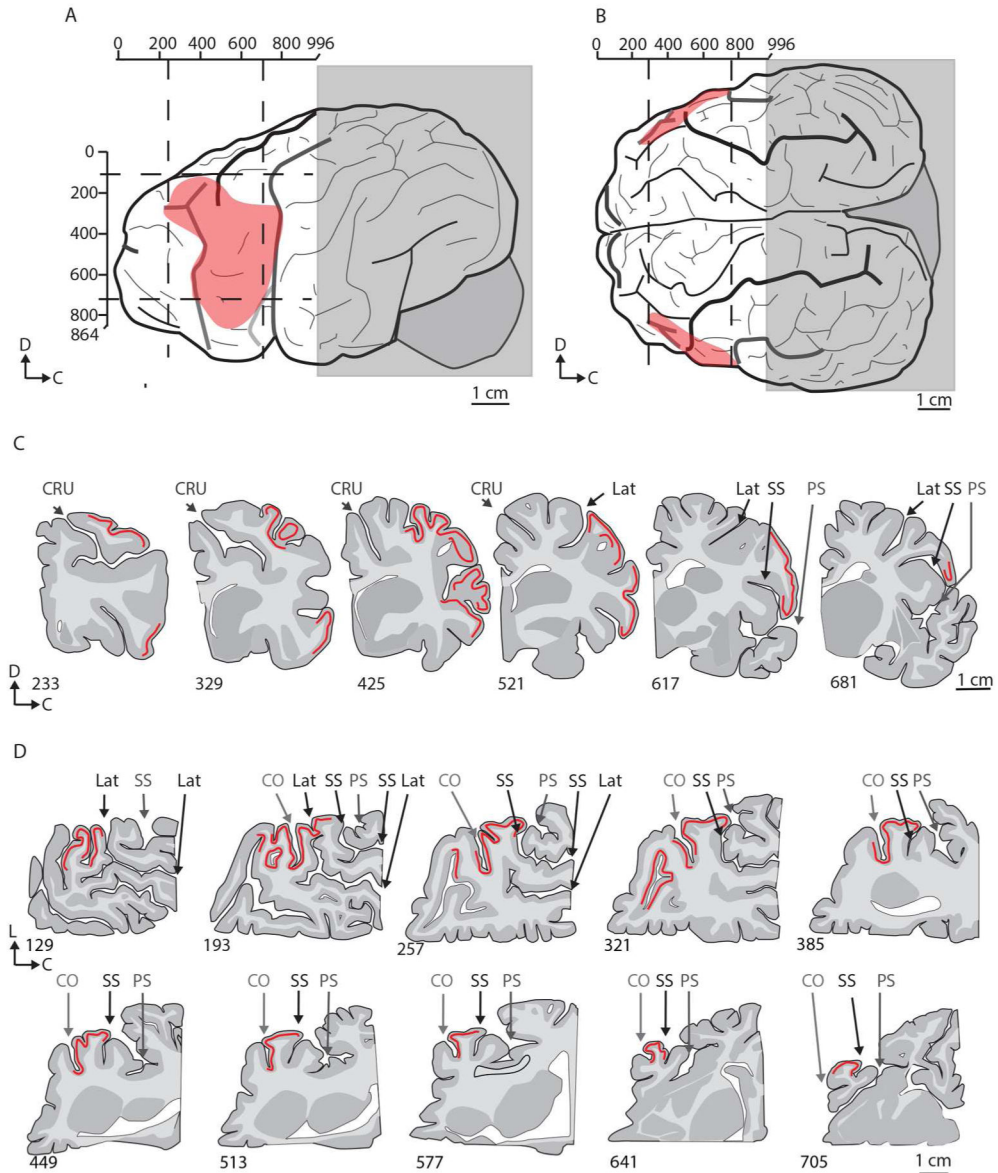


Figure 9.

The location of the presumptive somatosensory cortex. (A) and (B): Sketches of a lateral view and dorsal view of the cortex of a California sea lion. One hemisphere was cut in the coronal plane, and one in the horizontal plane. The area shaded in grey was not examined in this study. The numbered bars on the margins of the sketches indicate the numbering of the 50 μm sections that comprise the area that was examined. The red overlay indicates the area that where histological and cytoarchitectural markers of primary sensory cortex were revealed (as shown in figure 9). Note that there are some variations in the sulcal pattern between individuals and between hemispheres in the same individual. (C) and (D): Schematic of coronal sections (C) and horizontal sections (D), with the area where there were histological and cytoarchitectural markers of primary sensory cortex marked with a red stripe. The number of the section is indicated at the lower left. Arrows point to major sulci.

Abbreviations: C= caudal; Co= coronal sulcus, Cr= cruciate sulcus, D= dorsal, L= lateral, Lat= lateral sulcus, Ps= pseudosylvian, SS= suprasylvian sulcus.

Author Manuscript

Author Manuscript

Author Manuscript

Author Manuscript

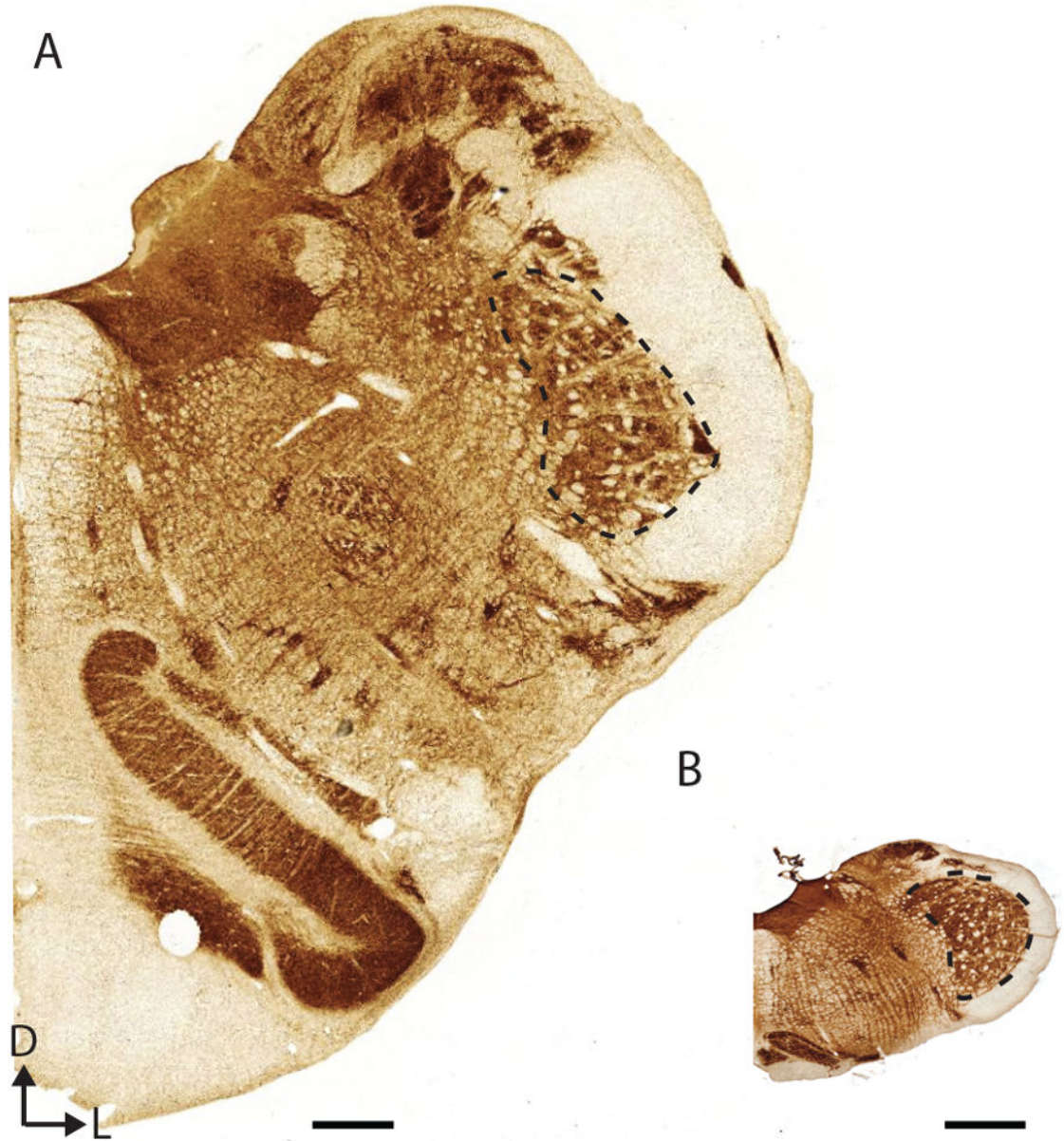


Figure 10. The comparative size of a sea lion and a rat brainstem. **(A)** A section of a sea lion brainstem at the level of the caudal SpVi. **(B)** A section of an adult rat brainstem at the same level. Scale bar = 1 mm. Abbreviations: D= dorsal, L= lateral.

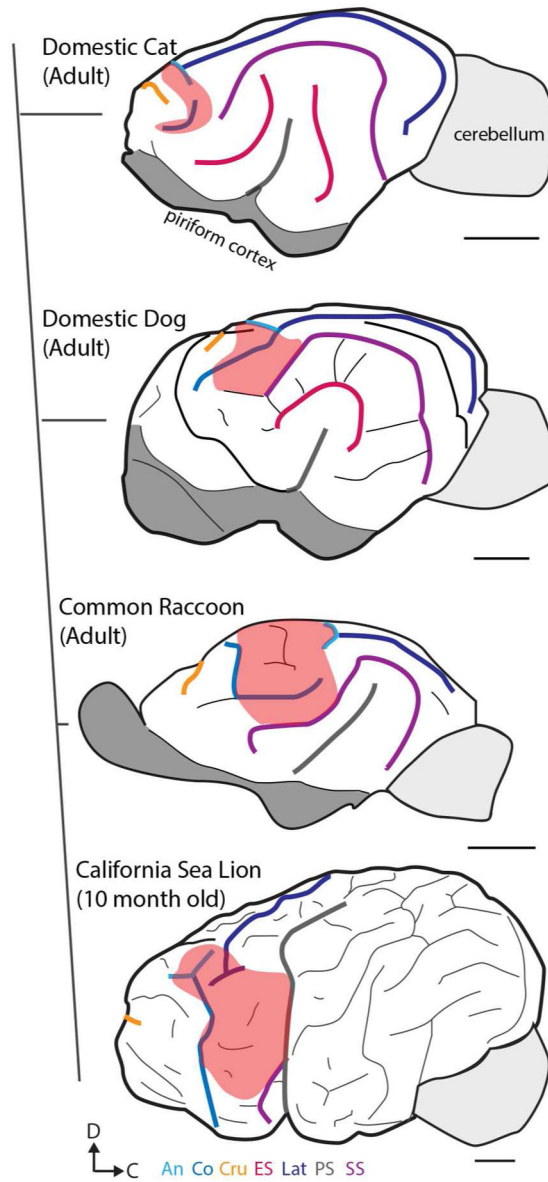


Figure 11.

Sketches of the lateral view of several carnivore brains, organized with a caldogram. The branched line to the left of the figure is based on Agnarsson et al. (2010). The branching pattern indicates clades, but the branch length does not indicate phylogenetic distance. The sulcal pattern shifts across species but the sulci bordering S1 are consistent. The sulcal pattern of the cat, dog and raccoon brains are based off of Snider and Niemer (1961), Singer (1962), Welker and Seidenstein (1959) and Rasmusson (1982). In the cat, dog and raccoon, S1 (as defined by electrophysiological mapping) is shaded in red. The area for S1 in the cat comes from Dykes et al. 1980 and Felleman et al. 1983, S1 in the dog from Bromiley et al. 1956, and S1 in the raccoon is from Welker and Seidenstein (1959) and Rasmusson (1982). S1 in the sea lion is from the results of this study. Note that the suprasylvian sulcus (SS) in the sea lion is found folded within the pseudosylvian fissure. Scale bar = 1 cm.

Abbreviations: Ans= ansate sulcus C= caudal; Co= coronal sulcus, Cr= cruciate sulcus; D= dorsal, ES= ectosylvian sulcus, Lat= lateral sulcus, Ps= pseudosylvian sulcus.

Author Manuscript

Author Manuscript

Author Manuscript

Author Manuscript

Table 1

Antigen	Description of Immunogen	Source, Host Species, Cat. #, Clone or Lot#, RRID	Concentration ($\mu\text{g/ml}$)
Vesicular glutamate transporter 1 (VGLUT1)	Recombinant protein from rat (aa 456–560)	Synaptic Systems, rabbit polyclonal, 135 303, AB_887876	0.2
Vesicular glutamate transporter 2 (VGLUT2)	Recombinant protein from rat VGLUT2	Millipore, mouse monoclonal, MAB5504, AB_2187552	0.2
Biotinylated horse anti-mouse IgG	Mouse IgG	Vector, mouse polyclonal, BA-2000, AB_2313581	3
Biotinylated goat anti-rabbit IgG	Rabbit IgG	Vector, rabbit polyclonal, BA-1000, AB_2313606	3

Author Manuscript

Author Manuscript

Author Manuscript

Author Manuscript